

Fuel cell control systems: a practical case

J. M. Andújar, F. Segura, M. J. Vasallo

Department of Electronic, Computer Science and Automatic Engineering, E.P.S., Huelva University
Carretera Huelva-La Rábida s/n, 21071 Palos de la Frontera (Spain)
phone:+34 959 217380, fax:+34 959 217348,
e-mail: andujar@diesia.uhu.es , francisca.segura@diesia.uhu.es , manuel.vasallo@diesia.uhu.es

Abstract

This work proposes and justifies an easy electric model of a power generation system based on a PEM fuel cell, the Nexa™ Power Module of Ballard. This model has been developed by means of experimental data obtained in our laboratory. Moreover, as this system generates unregulated power, a DC/DC converter is designed and a control system based on state feedback is proposed. This control system guarantees that fuel cell system operates at maximum power point taking into account the limits current slope of power module because of the slow response of auxiliary mechanics components.

Both the proposed electric model and the proposed control system, can be applied to any other PEM fuel cell system if the polarization curve along the whole output current range and the maximum power point is known.

Key words

Fuel cell, Nexa power module, feedback state, control, maximum power.

1. Introduction

PEM fuel cell power modules have unique features as compared with other fuel cell types. For example, relatively low operating temperature, the use of a solid polymerer, and high modularity. Moreover, these fuel cell systems are a viable alternative in areas where noise, vibration or emissions are of concerns. Although they are still more expensive in comparison with most power generation systems, advances in research, technology and reduction in the cost of producing hydrogen, are obtaining PEM fuel cells more competitive and popular in various applications.

Each power module requires its own auxiliary devices control system (hydrogen and oxygen supply and heat exchanger system) and control system of the fuel cell operating point [1]. In this work, first, an easy electric model of a fuel cell power system is presented. Then, a control system based on state feedback is proposed, which guarantees that the fuel cell system operates at maximum power point. For a practical case, the control system is designed for the Nexa™ Ballard Power System. Nevertheless, the proposed control system can be applied to any other PEM fuel cell system if the polarization curve around the maximum power point is known.

This work is organized as follow. In section 2, the Nexa™ Ballard system (mechanical and electrical characteristics) is described. In section 3, the developed experimental electrical model of this system is presented. In section 4, the control system is proposed and the simulation results are showed. In section 5, some conclusions are done.

2. Nexa™ PEM fuel cell power module

The Nexa™ Ballard Power System. is capable of providing 1.2kW of unregulated DC output. The output voltage level can vary from 43V at no load to about 26V at the full load. The stack is composed of 48 single cells connected in series. The operating temperature in the stack is around 65 °C at full load. The fuel is 99.99% hydrogen. Oxygen comes from the ambient air. The air is humidified through a built-in humidity exchanger to maintain membrane saturation and to prolong the life of the membrane. There is a small compressor supplying oxidant air to the fuel cell, and the speed of this compressor is adjusted by a internal controller to match the power demand from the fuel cell stack. The system is air-cooled (Fig. 1).

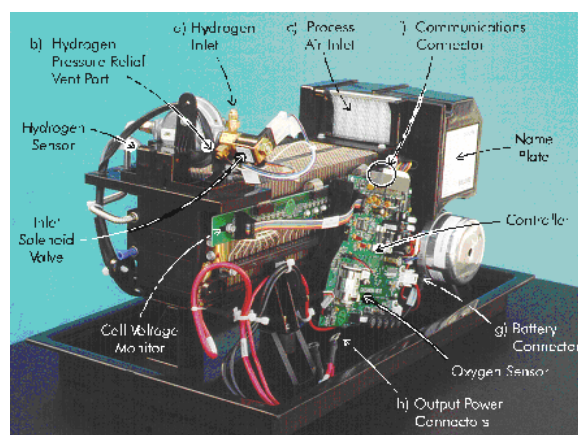


Figure 1. Nexa™ Power module.

When a step load change happens (Fig. 2), a 2.5 V drop in the output voltage is observed for a few hundreds of ms. This output voltage drop is related to a output power drop, that is produced because the compressor has a slow response. Furthermore, this transitory period can damage the fuel cell operation. Therefore, it is important to limit the current variation of the fuel cell system both if the fuel cell is working alone and is working with any other auxiliary source. If the power module is working alone, the load can not show supplied its own power demand. If there is an auxiliary source, this one must supply the load

power peak. Consequently, to avoid the damage to fuel cell operation, it is necessary to control its current output slope. In many applications, the fuel cell must work with slow variations in its current. Its behaviour can be described suitably by a stationary model. That is, one model which allows calculate the voltage and current values at any operation point of the polarization curve, but can not describe the transitory between neither couple of operation points. Therefore, this model is used, together with the converter model and the load model, to generate the whole plant model necessary to design the control system of the fuel cell operation point.

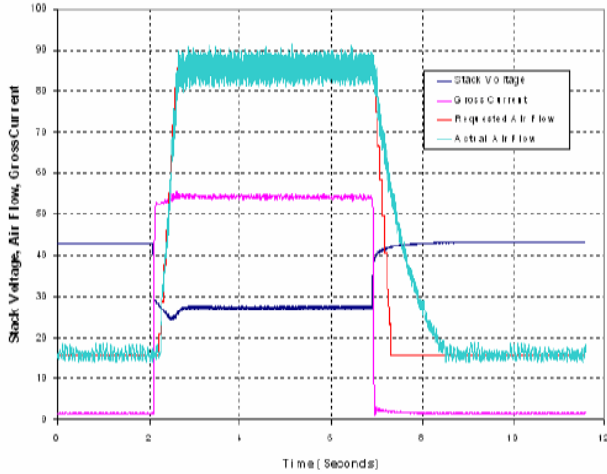


Figure 2. Fuel cell system response to load changes.

To obtain the maximum electric generation of the fuel cell system, the system has to work at maximum power point (1200 W, 26 V). The operation temperature is supposed to be constant, as it is regulated by the internal temperature control system. A DC/DC converter steps up the low output fuel cell voltage to the standard automotive DC bus 42 V [2]. The control system must maintain the operating point when there are perturbations in state variables of the system.

3. Nexa™ PEM fuel cell power module equivalent model

To obtain the equivalent electrical model of power module, we have carried out experimental studies in our laboratory (Fig. 3) with the Nexa™ Ballard power system. Figure 4 shows the electrical circuit scheme to obtain the polarization curve of the fuel cell system. The resistance variable (R_{load}) has been implemented by a resistances net connected in parallel, where we can select the resistance equivalent value with only put 'off' or 'on' the different switches (Fig. 5). The internal resistance value (R_{int}) can be calculated by equation (1).

$$R_{int} = \frac{E_o - V_{fc}}{I_{fc}} \quad (1)$$

Where:

E_o is the open circuit voltage, $E_o = 42$ V,
 V_{fc} is the output voltage, varies with R_{load} ,
 I_{fc} is the output current.



Figure 3. Power supply system based on Nexa™ Ballard module in our laboratory.

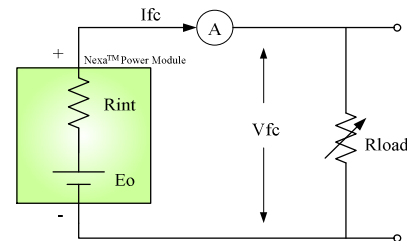


Figure 4. Scheme to measure the internal equivalent resistance (R_{int}).



Figure 5. Resistances net to measure the internal equivalent resistance (R_{int}).

The experimental data obtained are collected in tables I, II and III for different hydrogen supplied pressures, $P_{H_2} = 6$ atm, 10 atm and 12 atm.

TABLE I - $P_{H_2} = 6$ atm

$R_{load} (\Omega)$	$V_{fc} (V)$	$I_{fc} (A)$
4,70	36,6	7,53
2,35	34,2	14, 01
1,56	32,8	20,04
1,17	31,4	25,44
0,94	30,2	30,42
0,78	29,1	34,97
0,67	28,1	39,28
0,58	27,2	43,57

TABLE II - $P_{H_2} = 10 \text{ atm}$

$R_{load} (\Omega)$	$V_{fc} (V)$	$I_{fc} (A)$
4,70	36,7	7,55
2,35	34,5	14,17
1,56	32,8	20,10
1,17	31,3	25,44
0,94	29,8	30,42
0,78	28,7	34,72
0,67	27,7	39,02
0,58	26,8	42,72

TABLE II - $P_{H_2} = 10 \text{ atm}$

$R_{load} (\Omega)$	$V_{fc} (V)$	$I_{fc} (A)$
4,70	36,7	7,57
2,35	34,5	14,12
1,56	32,8	20,04
1,17	31,2	25,36
0,94	30	30,21
0,78	28,5	34,34
0,67	27,4	38,57
0,58	26,6	42,89

The values obtained for R_{int} at 65°C and different values of hydrogen supply pressure are showed in figure 6. We can assume that the internal equivalent resistance does not vary with hydrogen supplied pressure. An adjustment is done with experimental data and it is observed that R_{in} can be calculated by equation (2).

$$R_{int} = A_R + R_o \exp\left(\frac{-I_{fc}}{\tau_R}\right) - B_R \ln(I_{fc}) \quad (2)$$

Where $A_R = 0.82$, $B_R = 0.13$, $R_o = 0.8$ y $\tau_R = 5$.

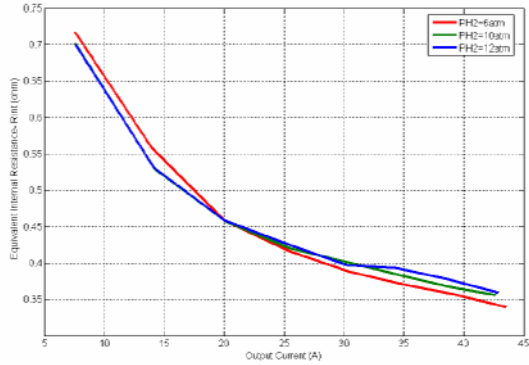


Figure 6. Relationship between R_{int} and fuel cell output current.

4. Control system

A. Plant description

As it is mentioned above, the fuel cell system is connected with a DC/DC converter. This converter regulates the output fuel cell voltage. The control signal is the converter duty cycle.

To design the control system, it must be taken in account the no-linearity of the all system. The approximate linearization technique allows to obtain a state lineal

model which shows the perturbations around the operation point [1].

Figure 7 shows electrical connection scheme between fuel cell system and DC/DC converter, taking into account parasite leaks in inductor and capacitor elements.

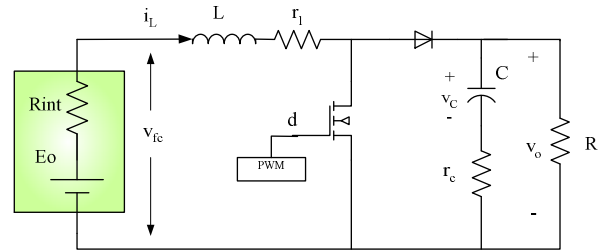


Figure 7. Connection electrical scheme between fuel cell system and DC/DC converter.

Analyzing the circuit when the switch is 'on' (Fig. 8), we obtain the equation (3) and (4).

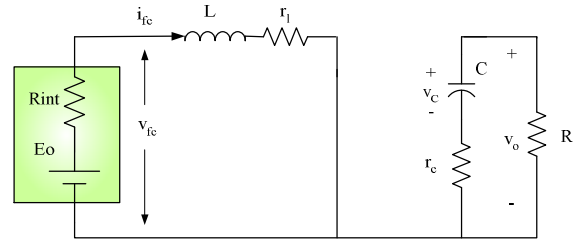


Figure 8. Connection electrical scheme between fuel cell system and DC/DC converter when switch is 'ON'.

$$\begin{bmatrix} \dot{i}_L \\ \dot{v}_C \end{bmatrix} = \begin{bmatrix} -\frac{r_L}{L} & 0 \\ 0 & -\frac{1}{C(R+r_c)} \end{bmatrix} \begin{bmatrix} i_L \\ v_C \end{bmatrix} + \begin{bmatrix} \frac{1}{L} \\ 0 \end{bmatrix} [v_{fc}] \quad (3)$$

$$v_o = \begin{bmatrix} 0 & \frac{R}{R+r_c} \end{bmatrix} \begin{bmatrix} i_L \\ v_C \end{bmatrix} \quad (4)$$

When the switch is 'off' (Fig. 9), we obtain the equation (5) and (6).

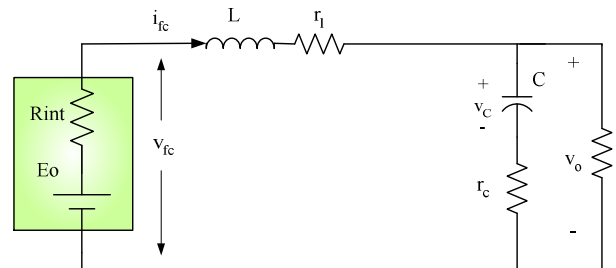


Figure 9. Connection electrical scheme between fuel cell system and DC/DC converter when switch is 'OFF'.

$$\begin{bmatrix} \dot{i}_L \\ \dot{v}_C \end{bmatrix} = \begin{bmatrix} -\frac{(1-d)}{L} \left(r_L + \frac{R \cdot r_c}{R+r_c} \right) & -\frac{1}{L} \frac{R(1-d)}{R+r_c} \\ \frac{1}{C} \frac{R(1-d)}{R+r_c} & -\frac{(1-d)}{C(R+r_c)} \end{bmatrix} \begin{bmatrix} i_L \\ v_C \end{bmatrix} + \begin{bmatrix} \frac{1}{L} \\ 0 \end{bmatrix} [v_{fc}] \quad (5)$$

$$v_o = \begin{bmatrix} \frac{R \cdot r_c}{R+r_c} (1-d) & \frac{R}{R+r_c} (1-d) \end{bmatrix} \begin{bmatrix} i_L \\ v_C \end{bmatrix} \quad (6)$$

With equations (3)-(6) we can obtain the converter average values state model, given by (7) and (8).

$$\begin{bmatrix} \dot{i}_L \\ \dot{v}_C \end{bmatrix} = \begin{bmatrix} -\frac{1}{L} \left(r_i + \frac{R \cdot r_c}{R + r_c} (1-d) \right) & -\frac{1}{L} \frac{R}{R + r_c} (1-d) \\ \frac{1}{C} \frac{R}{R + r_c} (1-d) & -\frac{1}{C(R + r_c)} \end{bmatrix} \begin{bmatrix} i_L \\ v_C \end{bmatrix} + \begin{bmatrix} \frac{1}{L} \\ 0 \end{bmatrix} v_{fc} \quad (7)$$

$$v_o = \begin{bmatrix} \frac{R \cdot r_c}{R + r_c} (1-d) & \frac{R}{R + r_c} \end{bmatrix} \begin{bmatrix} i_L \\ v_C \end{bmatrix} \quad (8)$$

We assume perturbations around operating point in the state, input and output variables, equation (9). The instantaneous fuel cell output voltage, v_{fc} , is related with i_{fc} , R_{int} and E_o in the same way as equation (1). Then, to obtain an expression for v_{fc} like a sum with a constant term (the operating point value) and another term varying with the perturbation, we must consider the dependence of R_{in} with i_{fc} . Therefore, we can express v_{fc} with the equation (10).

$$\begin{aligned} i_L &= I_L + i_{L\delta} \\ v_C &= V_C + v_{C\delta} \\ d &= D + d_\delta \end{aligned} \quad (9)$$

$$\begin{aligned} v_o &= V_o + v_{o\delta} \\ v_{fc} &= V_{fc} + v_{fc\delta} = \\ &= E_o - R_{int} I_{fc} + \\ &+ \left(A_R + R_o \exp\left(\frac{-I_{fc}}{\tau_R}\right) - B_R \ln(I_{fc}) \right) i_{fc} \\ &- \left(\frac{R_o}{\tau_R} \exp\left(\frac{-I_{fc}}{\tau_R}\right) + \frac{B_R}{I_{fc}} \right) i_{fc} \end{aligned} \quad (10)$$

The linealized model of complete system is obtained, and described by equation (11) [3],

$$\begin{bmatrix} \dot{i}_{L\delta} \\ \dot{v}_{C\delta} \end{bmatrix} = \mathbf{A}_\delta \begin{bmatrix} i_{L\delta} \\ v_{C\delta} \end{bmatrix} + \mathbf{B}_\delta \cdot d_\delta \quad (11)$$

$$v_{o\delta} = \mathbf{C}_\delta \begin{bmatrix} i_{L\delta} \\ v_{C\delta} \end{bmatrix} + \mathbf{D}_\delta \begin{bmatrix} v_{fc\delta} \\ d_\delta \end{bmatrix}$$

At maximum fuel cell power point, the values of voltage and current are 26 V and 46 A. The switching frequency is 50 kHz, the converter output voltage is 42 V and the input current and the output voltage ripple is 12% of the rated value. Then, it is obtained $D = 0.45$, $L = 58.96 \mu\text{H}$ and $C = 52.47 \mu\text{F}$. Figure 10, shows the adjustment between lineal and no lineal state model.

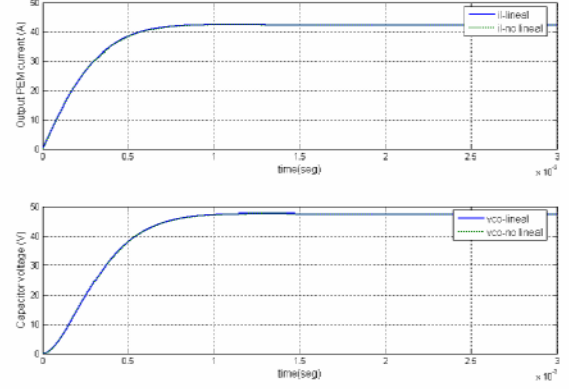


Figure 10. Matching between lineal and no-lineal model.

B. Control scheme

The control system must correct any state perturbation of the plant. Once it is proved that the plant is controllable, it must calculate the feedback state matrix (Fig. 11). This matrix comes fixed by the location of poles of linealized model in closed loop.

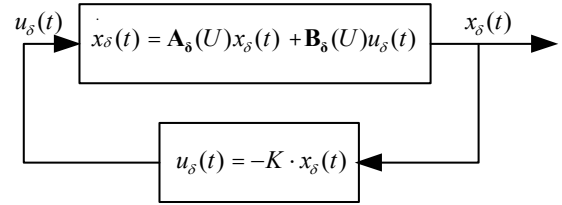


Figure 11. Lineal feedback of lineal system.

Poles of linealized system in closed loop are zeros of the characteristic equation (12).

$$|s\mathbf{I} - \mathbf{A}_\delta + \mathbf{B}_\delta \mathbf{K}| = (s^2 + 2\zeta\omega_n s + \omega_n^2) \quad (12)$$

Where the roots of equation (12) are expressed by expression (13).

$$s_{1,2} = -\zeta\omega_n \pm j\omega_n \sqrt{1 - \zeta^2} \quad (13)$$

In order to avoid a high overshoot and taking into account that there are not specifications in relation to speed of control system response, since it must avoid a fast transitory period, the damping coefficient is set at a value of $\zeta = 0.8$ and the settling time at $t_s = 0.01 \text{seg}$.

Since $t_s = \frac{4}{\zeta\omega_n}$, it be obtained that $\omega_n = 500$. The feedback state matrix results $\mathbf{K} = [-0.0105 \quad 0.0076]$.

To check the control system can correct any perturbation around the operation point, two different initial situation are considered for the simulations.

An initial perturbation of -5 V in capacitor voltage (v_C), is considered. Figure 12 shows as the control system increases the converter duty cycle until the error of state variable is zero.

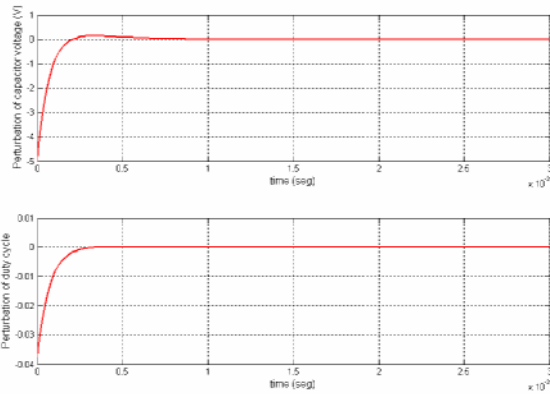


Figure 12. Behaviour of controlled system in closed loop (I).

If we consider a perturbation of -3 A in the second state variable, inductor current (i_L), figure 13 shows as the control system decreases the converter duty cycle until the error of state variable is zero.

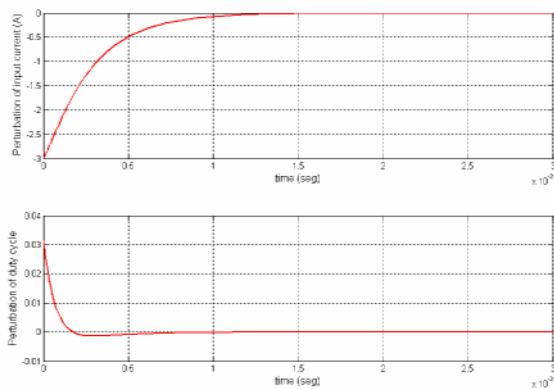


Figure 9. Behaviour of controlled system in closed loop (II).

5. Conclusions

This work presents and justifies the utility of a easy electrical static model of the fuel cell power generation Nexa™ Ballard. The parameters have been calculated to adjust the model to experimental data obtained in our laboratory. For the time being, most models available in scientific literature are electrochemist models with a great number of adjustable parameters which describe the behavior of certain type of fuel cell [4]. This model must be completed with the auxiliary devices models, but obtaining these models might be an unrealistic expectation due to proprietary reasons in such highly-engineered devices.

Moreover, the control system proposed guaranties that the system is working at maximum power point, with a regulated voltage at the output of DC/DC converter. Like this, we get; on the one hand, to have a controlled output voltage, and the other hand, avoids the power peaks caused by load transitory.

Future Works can be focused on to extend the system control to another operating point. In this way, if the system is working alone, we can establish an agreement

between fuel consumption an power generation. The other hand, if the system is working with another auxiliary power source, the fuel cell system can recharge this source without unnecessary leaks in efficiency.

References

- [3] Andújar Márquez J.M., Vasallo Vázquez M.J. Segura Manzano F., "A Suitable Model Plant for Control of the Set Fuel Cell-DC/DC Converter." *Journal of Renewable Energy*. (enviado).
- [1] Andújar Márquez J.M., Segura Manzano F., Vasallo Vázquez M.J., "A hybrid vehicle configuration with zero emission." *Proceedings of International Conference on Renewable Energies and Power Quality ICREPQ'2005*, pp. 147-148.
- [2] Andújar Márquez J.M., Vasallo Vázquez M.J. Segura Manzano F., "Un modelo orientado al control para un sistema pila de combustible." *XXVII Jornadas de Automática 2006*, pp. 538-546.
- [4] Corrêa J. M., Farret Felix A., Canha Luciane N., & Simões Marcelo G. "An Electrochemical-Based Fuel-Cell Model Suitable for Electrical Engineering Automation Approach." *IEEE Transactions on Industrial Electronics*, Vol. 51, pp. 1103-1111, 2004.